Fermi National Accelerator Laboratory

Vacuum Singularities in a Dual Multiperipheral Model

LOUIS A. P. BALÁZS[*]

Fermi National Accelerator Laboratory, Batavia, Illinois 60510

and

Physics Department, Purdue University, West Lafayette, Indiana 47907

ABSTRACT

We set up an explicit dual multiperipheral model, which is similar to the models of Huan Lee, Veneziano, and Chan and Paton, but explicitly takes into account the deferred thresholds arising from the production of resonance clusters. We assume that there are two such clusters, one with $(\text{mass})^2 \simeq 0.5 \text{ GeV}^2$ (ρ, ω, ϵ...) and the other with $(\text{mass})^2 \simeq 1.5$ GeV^2 (f, B, D, A_2...). At lower energies only the first plays any role, and we find that the total vacuum-state cross section $\sigma \propto s^{\alpha_{\hat{P}} - 1}$ on the average, where $\alpha_{\hat{P}} \simeq 0.85$. For $s \gtrsim 50 \text{ GeV}^2$, on the other hand, the second cluster also comes in, and σ flattens out. This behavior has all the features of the experimental data and is thus a completely satisfactory alternative to the conventional description in terms of the P and f. In addition, all of the parameters describing our vacuum singularities can be calculated a priori in our model, and are in reasonably good agreement with the data.

I. INTRODUCTION

During the past several years, multiperipheral models have been used extensively in describing high-energy phenomena, either directly, or as first order terms in more elaborate schemes. Most of these models, have been either purely phenomenological, or have been based on single pion exchange.[1] The latter, however, have had considerable difficulty in generating output Regge trajectories with sufficiently high intercepts.[2] It is clear that Reggeon exchanges also play an important role in high-energy production.

One of the most promising approaches to an understanding of high-energy scattering is the dual multiperipheral model. This was originally proposed by Huan Lee,[3] Veneziano,[4] and Chan and Paton.[5] Recently, more detailed calculations have been made by Chan, Paton, Tsou and Ng,[6] who also made additional duality assumptions. They find semi-quantitative agreement with experiment, and, in particular, are able to explain the small slope of the Pomeron trajectory in a natural way. One problem with all these approaches, however, has been that the f trajectory is not generated in the vacuum state along with the Pomeron (P).[7] We shall see, however, that if we take into account the thresholds resulting from the production of more than one resonance cluster, we generate a set of complex singularities whose net effect is to give a cross section very similar to the one given by the conventional P + f description below ISR energies. Some of our results were presented earlier.[8] In this paper we discuss them in more

detail and at the same time present additional results.

In Sec. II we review briefly the dual multiperipheral approach and in Sec. III we write down a specific model. In Sec. IV, the self-consistency requirement that the Reggeon be correctly reproduced is used to fix the parameters of our model. In Sec. V we use our model to generate the Pomeron in the case where only one type of cluster is produced; this gives a description which is valid only at moderate energies. In Sec. VI we consider a two-cluster version which is applicable at much higher energies. In Sec. VII we study the effect of the deferred threshold for the production of a higher-mass cluster; we find a cross section similar to one which is given by the conventional $P + f$. In Sec. VIII we estimate the effect of diffractive corrections at moderate energies and find that, although this changes the overall magnitude of our cross section, it does not change its energy dependence. Finally in Sec. IX we use our model to calculate the overall magnitude of the vacuum-state contribution to the pp cross section.

II. THE DUAL MULTIPERIPHERAL APPROACH

As in any multiperipheral scheme, we shall assume that the amplitude

for the production of clusters is given by diagrams of the type shown in

Fig. 1. By using multiparticle unitarity we obtain from these a two-body

absorptive part given by the sum of ladder diagrams of Fig. 2. In the

simplest multiperipheral models the horizontal lines are single Regge

exchanges α_e. In a dual multiperipheral model, on the other hand, they

are always linear combinations of exchange-degenerate sets of Regge

exchanges. According to the usual rules of quark-duality diagrams, two

kinds of diagrams can now arise:[6]

(A) If we are interested in generating Reggeons we only have uncrossed

(planar) quark-duality diagrams of the type shown in Fig. 3. The exchanges

then correspond to Regge propagators

$$R = e^{-i\pi\alpha_e(t)} s^{\alpha_e(t)} \tag{2.1}$$

This would arise, for example, if we have exchange-degenerate $\rho + f$

exchange.

(B) If we are interested in generating the Pomeron we must also

have crossed (nonplanar) loops of the type shown in Fig. 4. According

to the usual quark-diagram rules, the two Reggeons in a given loop must

either be both uncrossed or both crossed. In the latter case we then have

a Reggeon propagator

$$R = 1s^{\alpha_e(t)} \tag{2.2}$$

This would arise, for example, if we took the difference of exchange-

degenerate ρ and f exchange, a combination which would arise in the

exotic I = 2 state of $\pi\pi$ scattering. In the Chan et al.[6] and Chew and

Rosenzweig[7] approaches the uncrossed loops are summed first, and then

used as inputs in sums over crossed loops to generate the Pomeron.

In the present paper we shall sum over the uncrossed and crossed loops

simultaneously so that we have essentially a two-channel problem.

We will only consider the simple case of isospin symmetry (say,

$\pi\pi$ scattering). The crossed and uncrossed loops can then be written in

terms of the Chan-Paton factors[9] as $P_0 C$ and $(P_0 + P_1)U$ where P_0, P_1

are t-channel isospin I_t = 0, 1 projection operators and C and U are loop

integrals involving the factors (2.1) and (2.2), which are independent of

internal quantum numbers. Note that the crossed diagram contributes

only to I_t = 0 whereas the uncrossed diagrams contribute to both isospin

states.

The above picture of the Pomeron is, of course, somewhat oversimplified.

A more systematic approach would incorporate SU(3) and be based on the

1/N expansion of Veneziano.[10] We do not expect our results to be changed

very much by this, however.

In order to obtain an additional constraint on our model, we shall

make the assumption that the clusters (the vertical lines of Fig. 2) are

dual in a finite-energy sum rule (FESR) sense to Regge behavior. (see

Fig. 5). This sort of constraint on sums of ladder graphs was first used

a number of years ago in a pion-exchange model,[11] and has recently

been applied to the dual multiperipheral model by Chan, Paton, Tsou and

Ng.[6] If Γ represents the coupling of the cluster to the external Reggeon

lines of Fig. 5 it leads to a relation of the form

$$\Gamma(t_1, t_2, t_1', t_2', t) = F(t)g_1(t_1, t_1', t)g_2(t_2, t_2', t) \qquad (2.3)$$

where g_1 and g_2 are triple-Regge couplings and F is a purely kinematic

factor. We shall argue in Sec. IV that F is an approximately universal

factor, which is not only independent of the external Reggeon lines but

also of t_1, t_2, t_1', t_2'. We can therefore set $F = F(t)$. This means that

Γ factorizes, which permits us to simplify considerably the problem of

summing the diagrams of Fig. 2.

Although Eq. (2.3) gives a relation between Γ and $g_1 g_2$, it should

perhaps be emphasized that it does not actually correspond to replacing

Fig. 5(a) by 5(b), as was done in refs. 6 and 7. We find that the latter

approximation is too crude and, in particular, leads to a somewhat different

output singularity structure than the one obtained by our model.

III. A MULTIPERIPHERAL MODEL

The model we will consider is a standard multi-Regge model similar to that of Chew, Goldberger and Low[12] but applied to the production of clusters. Specifically we assume that the absorptive part A(t, s) of the process 12 → 1'2' is given by Fig. 6. If we assume that, except for the end clusters R and Q, only one type of narrow-resonance cluster of mass $\sqrt{s_a}$ is produced, A(t, s) is built up by linking the graphs of Fig. 5(a), which gives a contribution

$$V(t,s) = \Gamma_a \, \delta(s - s_a) \ . \tag{3.1}$$

We will take $s_a \simeq 0.5 \, \text{GeV}^2$, which corresponds to the ρ, ω, $\epsilon \ldots$ peaks, and assume that the horizontal lines of Fig. 6 correspond to the exchange of a single effective Reggeon with trajectory

$$\alpha_e(t) = 0.25 + t \ . \tag{3.2}$$

This can be thought of as some kind of average of the pion and the leading Reggeon with trajectory $\alpha = 0.5 + t$, both of which would contribute in a more realistic description.

The problem simplifies considerably if we take the Mellin transform of A

$$A(t, j) = \int_0^\infty ds \, s^{-j-1} A(t, s) \ . \tag{3.3}$$

From Eqs. (3.1) and (2.3)

$$V(t, j) = g(t_1 t_2 t)g(t_1' t_2' t)F_a(t)s_a^{-j-1} \quad . \tag{3.4}$$

We will consider the t-channel isospin $I_t = 0$ state, where g is the $\alpha_e - \alpha_e - f$ triple-Regge coupling. Since Eq. (3.4) factorizes, the diagrams of Fig. 6 are separable in the usual high-energy approximation and

$$A(t, j) = \gamma_{11'f}(t)s_R^{-j-1}F_R(t)B(t, j)F_Q(t)s_Q^{-j-1}\gamma_{22'f}(t) \tag{3.5}$$

where $\gamma_{11'f}$ and $\gamma_{22'f}$ are the 11'f and 22'f Regge couplings, $\sqrt{s_R}$, $\sqrt{s_Q}$ are the masses of R and Q, and

$$B(t, j) = K(t, j) + K(t, j)F_a(t)s_a^{-j-1}K(t, j) + \ldots, \tag{3.6}$$

as can be seen from Fig. 7 and Eq. (3.4). The function K(t, j) has the general structure

$$K(t, j) = \int gRRg \quad , \tag{3.7}$$

where R is given by Eq. (2.1) or (2.2). It has a logarithmic branch point at $j = \alpha_c(t) = 2\alpha_e(\frac{1}{4}t) - 1$, corresponding to double-Regge exchange. If we approximate this by a pole at $j = \alpha_c(t)$ we then have

$$K(t, j) = \frac{k(t)}{j - \alpha_c(t)} x(t)^{\alpha_c(t) - j} \quad . \tag{3.8}$$

The factor $x^{\alpha_c - j}$ is an effective threshold term, as can be seen by taking

the inverse Mellin transform of Eq. (3.8), which gives

$$K(t, s) = k(t)s^{\alpha_c(t)} \theta(s - x) , \qquad (3.9)$$

where θ is the usual step function. It arises from the fact that the momentum

transfers of the Regge exchanges are limited. This is shown explicitly

in Appendix A for the specific case of pion exchange ($\alpha_e = 0$) but is actually

true for a broad class of models. The function $k(t)$ has the form

$$k(t) = \int dt'dt''(-\lambda)^{-\frac{1}{2}} \theta(-\lambda)g^2(t', t'', t)X(t', t'') \qquad (3.10)$$

where $\lambda = t^2 + t'^2 + t''^2 - 2(tt' + tt'' + t't'')$, and X depends on the signature

factors.

Because of t_{min} effects, Eqs. (3.9) and (3.10) are actually a simplified

version of the true behavior of $K(t, s)$, which is more complicated for small

s. However, since this complicated region is relatively small, it should be

a reasonable average approximation if x is treated as an adjustable quantity,

at least for the purpose of obtaining the Mellin transform. This will be

discussed in more detail elsewhere.

Eq. (3.6) can be explicitly summed to give

$$B(t, j) = K(t, j)/D(t, j) \qquad (3.11)$$

where

$$D(t, j) = 1 - s_a^{-j-1} F_a(t) K(t, j) \qquad (3.12)$$

The function B will have a pole at $j = \alpha(t)$ if

$$D\Big(t, \alpha(t)\Big) = 0 \qquad (3.13)$$

The corresponding residue is then

$$c_\alpha^{\;2}(t) \;=\; K(t,\;\alpha)/\left[\,\partial D(t,\;\alpha)/\,\partial\alpha\right] \tag{3.14}$$

From Eq. (3.5) the corresponding residue of $A(t,\;j)$ is

$$b_{11',\;22'}(t) \;=\; \gamma_{11'\alpha}(t)\gamma_{22'\alpha}(t) \tag{3.15}$$

where

$$\gamma_{11'\alpha}(t) \;=\; \gamma_{11'f}(t)s_R^{\;-\alpha-1}F_R(t)c_\alpha(t), \tag{3.16}$$

and similarly for $\gamma_{22'\alpha}$.

IV. SELF-CONSISTENCY CONDITION FOR REGGEONS

If we are interested in generating Reggeons, only the propagators (2.1) come in and so

$$X(t',\;t'') \;=\; e^{\;i\pi\left[\alpha_e(t')\;-\;\alpha_e(t'')\right]} \tag{4.1}$$

in Eq. (3.10). Now triple-Regge fits[13] suggest that $g(t,\;t,\;0) \approx$ Constant for small t. We will go further and assume that $g(t',\;t'',\;t) \approx$ Constant. We can then evaluate the integral (3.10) by changing variables to u and z, where

$$t',\;t'' \;=\; u + \tfrac{1}{4}t \pm z(ut)^{\frac{1}{2}} \qquad, \tag{4.2}$$

so that $-\infty < u < 0$ and $-1 < z < 1$. Since the approximation $g^2 \approx$ Constant in fact breaks down for large momentum transfers we will put in a straight

cutoff in u at u = - τ. For small t, Eq. (3.10) then gives

$$k(t) = k_f(t) \equiv k_0 \left[1 + \tfrac{1}{2} \pi \tau t + O(t^2) \right] \quad .$$ (4.3)

We will fix k_0 and τ, as well as $x(0)$ and $x'(0)$, by the requirement

that Eqs. (3.13) and (3.16) are satisfied with $\alpha = \alpha_f = 0.5 + t$ and

$\gamma_{11'\chi} = \gamma_{11'f}$. Note that $\gamma_{11'f}$ then cancels in Eq. (3.16) giving

$$s_R^{-\alpha_f - 1} F_R(t) = c_f^{-1}(t)$$ (4.4)

Eqs. (3.13) and (4.4) are therefore conditions only on the internal couplings

of the model and would be the same irrespective of the external lines in

Fig. 6. From Eq. (4.4) this in turn means that $s_R^{-\alpha_f - 1} F_R(t)$ is a

universal function, independent of the external lines. In particular, if

the external lines are themselves Reggeons (as in Fig. 5) rather than

ordinary particles, this means that $F_R(t)$ must be independent of

t_1, t_2, t_1', t_2'.

Since $s_R^{-\alpha_f - 1} F_R(t)$ is independent of the external lines there is

no loss of generality if we restrict ourselves to $\pi\pi$ or Reggeon-Reggeon

scattering, for both of which R = a.

(A) In the case of $\pi\pi$ scattering, a conventional first-moment

finite-energy sum rule (FESR) gives

$$\int_0^N A(t, s) \nu \, d\nu = \gamma_{\pi\pi f}^2 N^{\alpha_f + 2} / (\alpha_f + 2)$$ (4.5)

where $\nu = \frac{1}{2}(s - u) \simeq s + \frac{1}{2}t$, and N is a point halfway between resonances.

If we restrict ourselves to a single narrow resonance at $s = s_a (= m_\rho^2)$,

A(t, s) is given by Eq. (3.1) and a comparison with Eq. (2.3) gives

$$F_a(t) \simeq (s_a + \tfrac{1}{2}t)^{-1} N^{\alpha_f + 2} / (\alpha_f + 2) \qquad (4.6)$$

with $N = 2s_a + \frac{1}{2}t$, the point halfway between the ρ and f resonances. If

we now impose the conditions (3.13) and (4.4) with $\alpha = \alpha_f$ and R = a, we

obtain $k_0 = 2.50$, $\tau = 0.54$, $x(0) = 7.1$ and $x'(0) = 1.73 \ x(0)$.

(B) For $\alpha_e - \alpha_e$ scattering (Fig. 5) we used an approximate version

of an FESR in which we essentially integrated over the external momentum

transfers and dropped logarithmic terms. We then have

$$F_a(t) \simeq s_a^{\alpha_c(t)} N^{\alpha - \alpha_c + 1} / (\alpha - \alpha_c + 1) \qquad (4.7)$$

with $N \simeq 2s_a$ if we set $\nu \approx s$. This time we obtain $k_0 = 1.92$, $\tau = 0.39$,

$x(0) = 5.4$ and $x'(0) = 0.69 \ x(0)$. We will see that our final results will

not depend too much on the prescription we use.

V. POMERON PARAMETERS IN THE ONE-CLUSTER MODEL
AND MODIFIED f/P UNIVERSALITY

If we wish to generate the Pomeron in the t-channel, we must include

the non-planar graphs of Fig. 4 in addition to the planar graphs of Fig. 3,

and so, from Eqs. (2.1) and (2.2),

$$X(t', t'') = 1 + e^{i\pi\left[\alpha_e(t') - \alpha_e(t'')\right]} \tag{5.1}$$

in Eq. (3.10). If we make the same assumptions as in Sec. IV, Eq.

(3.10) then gives

$$k(t) = k_P(t) \equiv k_0\left[2 + \tfrac{1}{2}\pi\tau t + 0(t^2)\right] \tag{5.2}$$

where k_0 and τ, as well as $x(0)$ and $x'(0)$ are the same as in Sec. IV.

The Pomeron $(\hat{P})$ trajectory is now given by Eq. (3.13) with

$\alpha = \alpha_{\hat{P}}$ and the corresponding coupling by Eq. (3.16), which gives

$$\gamma_{11'\hat{P}}(t) = \gamma_{11'f}(t) s_R^{-\alpha_{\hat{P}} - 1} F_R(t) c_{\hat{P}}(t). \tag{5.3}$$

In the case of $\pi\pi$ scattering, for example, where $R = a$, the prescription

(4.6) gives

$$\alpha_{\hat{P}}(t) = 0.83 + 0.37t + 0(t^2) \tag{5.4}$$

and

$$\gamma^2_{\pi\pi\hat{P}}(0) = 1.41 \gamma^2_{\pi\pi f}(0) \tag{5.5}$$

Prescription (4.7), on the other hand, gives

$$\alpha_{\hat{P}}(t) = 0.87 + 0.37t + 0(t^2)$$ (5.6)

and

$$\gamma^2_{\pi\pi\hat{P}}(t) = 1.50\left[1 - 0.79t + 0(t^2)\right]\gamma^2_{\pi\pi f}(t).$$ (5.7)

These results are fairly close to each other.

Eqs. (5.5) and (5.6) both give trajectory slopes which are much smaller than those for the Reggeon. This result is one of the main successes of the dual multiperipheral model and follows from the relative t dependences of Eqs. (4.3) and (5.2). Previous multiperipheral models gave excessively large Pomeron slopes.

There is only one real solution to Eq. (3.13) with $\alpha = \alpha_{\hat{P}} > 0$. This means that we do not generate an output f trajectory along with the Pomeron. On the other hand, the latter has an intercept at $\alpha_{\hat{P}}(0) \simeq 0.85$ rather than at $\alpha_{\hat{P}}(0) = 1$. It must therefore be considered as some kind of average of the conventional P and f. The extensive phenomenological fits of Dash and Bali[14] show that this kind of trajectory is quite capable of accounting for the data at moderate energies. It fails, of course, at higher energies, but we shall see that other effects come in in this region.

If we combine Eqs. (5.3) and (4.4) we obtain

$$s_R^{\alpha_{\hat{P}} - \alpha_f}\gamma_{11'\hat{P}}(t)/\gamma_{11'f}(t) = c_{\hat{P}}(t)/c_f(t) ,$$ (5.8)

a result which is independent of $F_R(t)$. Since $c_{\hat{P}}/c_f$ is independent of

the external lines, Eq. (5.8) is in effect a generalized version of f/P

universality[15]; in the conventional version the factor $s_R^{\alpha_{\hat{P}} - \alpha_f}$ does not

come in. We can therefore obtain the $\hat{P}/f$ ratio from the corresponding

ratio for $\pi\pi$ scattering, where $R = a$. Thus

$$\gamma_{11'\hat{P}}(t)/\gamma_{11'f}(t) = (s_R/s_a)^{\alpha_f - \alpha_{\hat{P}}} \gamma_{\pi\pi\hat{P}}/\gamma_{\pi\pi f} \qquad (5.9)$$

For pp scattering the cluster R is presumably the nucleon and so $s_R = m_p^2$.

VI. POMERON PARAMETERS IN THE TWO-CLUSTER MODEL

Up to now we have only considered the production of a single type of

cluster of $(\text{mass})^2 = s_a \simeq 0.5 \text{ GeV}^2$. Suppose now that we have a second

cluster of $(\text{mass})^2 = s_b = 1.5 \text{ GeV}^2$, which corresponds to the f, B, D

and A_2 resonances. We must then replace Eq. (3.1)

$$V(t, s) \rightarrow \Gamma_a \delta(s - s_a) + \Gamma_b \delta(s - s_b) , \qquad (6.1)$$

which in turn means that we must make the replacement

$$s_a^{-j - 1} F_a(t) \rightarrow s_a^{-j - 1} F_a(t) + s_b^{-j - 1} F_b(t) \qquad (6.2)$$

in Eqs. (3.4), (3.6) and (3.12).

The factor $F_b(t)$ can also be calculated by considering either $\pi\pi$

or Reggeon-Reggeon scattering.

(A) If we take the difference between an FESR (4.5) with $N = 4s_a + \frac{1}{2}t$, which is midway between the f and g resonances and one with $N = 2s_a + \frac{1}{2}t$, which is midway between the ρ and f resonances, we obtain

$$F_b(t) = (s_b + \tfrac{1}{2}t)^{-1}\left[(4s_a + \tfrac{1}{2}t)^{\alpha_f + 1} - (2s_a + \tfrac{1}{2}t)^{\alpha_f + 1}\right]/(\alpha_f + 1) \qquad (6.3)$$

(B) If we follow the same procedure for Reggeon-Reggeon scattering, we have, instead,

$$F_b(t) \simeq s_b^{\alpha_c(t)}\left[(4s_a)^{\alpha - \alpha_c + 1} - (2s_a)^{\alpha - \alpha_c + 1}\right]/(\alpha - \alpha_c + 1) \qquad (6.4)$$

We will see in Sec. VII that the second cluster (b) does not contribute at intermediate energies. We therefore expect the one-cluster results of Sec. IV for the parameters k_0, τ, $x(0)$, $x'(0)$ to continue to apply, since Reggeons are important only at those energies. On the other hand, both clusters must be included if we want to calculate the Pomeron (P) at very high energies. If we therefore take R = a, and use Eqs. (3.13), (3.16), (5.2) and (6.2) with $\alpha = \alpha_P$, and Eqs. (4.7) and (6.4) for F_a and F_b (Prescription B), we obtain

$$\alpha_P(t) = 0.98 + 0.38t + 0(t^2) \qquad (6.5)$$

and

$$\gamma_{\pi\pi P}^2(t) = 1.50\left[1 - 0.79t + 0(t^2)\right]\gamma_{\pi\pi f}^2(t) \qquad (6.6)$$

for $\pi\pi$ scattering. It is straightforward to show that a modified f/P
universality continues to hold, with

$$\gamma_{11'P}(t)/\gamma_{11'f}(t) = (s_R/s_a)^{\alpha_f - \alpha_P} \gamma_{\pi\pi P}/\gamma_{\pi\pi f} \qquad (6.7)$$

instead of Eq. (5.9). Eq. (6.7) then permits us to calculate the P/f
ratio for any other process.

In the above calculation we continued to assume that there is only
one end cluster A. At high energies, we may expect more. If so, we must
make the replacement

$$s_R^{-j-1} F_R(t) \rightarrow \sum_R s_R^{-j-1} F_R(t)$$

and similarly for Q. This would change our couplings but not our trajectory
α_P.

The trajectory intercept in Eq. (6.5) is higher than in the one-cluster
case, although the slope is not very different. It should be emphasized,
however, that this trajectory is only relevant asymptotically. In the
next section we will investigate what happens at finite energies for pp
scattering.

VII. THRESHOLDS OF THE POMERON

Up to now we have only considered the leading (real) j-singularities

generated by our models. However, because of factors like $(s_a x)^{-j}$ in

the D functions, we also have an infinite set of complex poles in the

j-plane. These in turn lead to oscillating cross sections at intermediate

energies, as discussed by Chew, Snider and Koplik.[16]

(a) In the one-cluster model, an alternative way of seeing how

oscillations arise is to directly take the Mellin transform of Eq. (3.5)

with B given by Eqs. (3.6) and (3.8). The individual terms in the expansion

(3.6) then lead to thresholds in A at $s = s_R^2 x$, $s_R^2 x^2 s_a$, ..., corresponding

to the production of 0, 1, ... a-clusters. Since s_a is small, the resulting

oscillations damp out fairly rapidly as we go up in energy and should be

negligible in the region where Regge phenomenology is normally applied.

It is therefore a good approximation to keep only the leading singularity,

so that

$$B = B_P^\Lambda(t, j) \simeq \frac{c_P^\Lambda{}^2(t)}{j - \alpha_P^\Lambda} x^{\alpha_P^\Lambda - j} \qquad (7.1)$$

The factor $x^{\alpha_P^\Lambda - j}$ was inserted to guarantee that the threshold of $B(t, s)$

occurs at $s = x$, as required by Eqs. (3.6), (3.8) and (3.9).

(b) In the two-cluster model, additional thresholds arise from the

production of b clusters. We shall see that the first such threshold occurs

in a region where a Regge description is normally used and where any

oscillations arising from the a-clusters have already damped out. We shall also see that it does have an important effect on the energy dependence of the cross section. The oscillations arising from any subsequent thresholds will be seen to be negligible, however.

In the case of pp scattering, we must replace Eq. (3.5) by

$$A(t, j) = \gamma^2_{ppf}(s_R^2)^{-j-1}F_R^2(t)B_P(t, j) \qquad (7.2)$$

where R is a baryon, and B_P is given by the diagrams of Fig. 8. If we again apply the duality relation (2.3)(Fig. 5) we have

$$B_P(t, j) = B_{\hat{P}}^{\wedge}(t, j) + B_{\hat{P}}^{\wedge}(t, j)F_b(t)s_b^{-j-1}B_{\hat{P}}^{\wedge}(t, j) + \ldots \qquad (7.3)$$

If we now make the approximation (7.1) for the one-cluster function $B_{\hat{P}}^{\wedge}$, and use Eq. (5.3) we obtain

$$A(t,j) = \gamma^2_{pp}\hat{P}(t) \left\{ \frac{(s_R^2 x)^{\alpha_{\hat{P}}^{\wedge} - j}}{j - \alpha_{\hat{P}}^{\wedge}} + \eta(t)\frac{(s_R^2 x^2 s_b)^{\alpha_{\hat{P}}^{\wedge} - j}}{(j - \alpha_{\hat{P}}^{\wedge})^2} + \ldots \right\} \qquad (7.4)$$

where

$$\eta(t) = c_{\hat{P}}^2(t)s_b^{-\alpha_{\hat{P}}^{\wedge} - 1}F_b(t) \qquad (7.5)$$

The Mellin transform of Eq. (7.4) gives

$$A(t, s) = \gamma_{pp}\hat{P}^2(t)s^{\alpha_{\hat{P}}^{\wedge}} \left\{ \theta(s - s_R^2 x) + \eta \ln(s/s_R^2 x^2 s_b^2)\theta(s - s_R^2 x^2 s_b) + \ldots \right\}$$

$$(7.6)$$

so that we have thresholds at $s = s_R^2 x$, $s_R^2 x^2 s_b$, ... corresponding to

the production of 0, 1, ... b-clusters.

In Fig. 8 we plot the total cross section $\sigma \simeq s^{-1} A(0, s)$ obtained

from Eq. (7.6). The solid line corresponds to taking $s_R \simeq m_p^2$ and

using Eqs. (4.6) and (6.3) (Prescription A) whereas the dashed line

corresponds to taking $s_R \simeq 1$ GeV^2 and using Eqs. (4.7) and (6.4) (Prescription

B). These are compared with the experimental $\frac{1}{2}(\sigma_{pp} + \sigma_{p\bar{p}})$, a combination

which is essentially the vacuum-state contribution to the pp cross section

and would conventionally be described by P + f. We see that our description

is equally acceptable. For $s < s_R^2 x^2 s_b$ ($\simeq 45$ GeV^2), $\sigma \propto s^{\alpha_P^\Lambda(0) - 1}$ with

$\alpha_P^\Lambda(0) \simeq 0.87$ which lies between the conventional $\alpha_P(0)$ and $\alpha_f(0)$, whereas

for $s > s_R^2 x^2 s_b$ we have a cross section which is well approximated by

its asymptotic behavior $\sigma \propto s^{\alpha_P(0) - 1}$ with $\alpha_P(0) \simeq 0.98$ (using Prescription

B). It should perhaps be emphasized that the rather sharp threshold

in our model is not an essential feature of our approach and would be

smoothed out in a more realistic model, e.g. one with additional end

clusters, or clusters with some spread in their mass.

We could always add in a third cluster c in our model, with

$s_c \simeq 2.5$ GeV^2, which would correspond to the g, ρ', A_3 and $\omega(1675)$

peaks. It is not clear that this would be a valid procedure, however, since

such a state is presumably already included in some average way in the

aa state and double-counting may occur.[17] If we nevertheless include it

we obtain the dotted line of Fig. 8 instead of the corresponding solid line.

In Fig. 8, the overall magnitude (or $\gamma_{pp\hat{P}}^2$) was fitted to the data, but the shape is completely predicted in our model. In Sec. IX we will also calculate this overall magnitude.

VIII.   DIFFRACTIVE CORRECTIONS

Up to now we have only considered the multiperipheral component of the Pomeron and have completely ignored the effect of diffractive corrections. A complete treatment of this would have to involve the full machinery of the Veneziano $1/N$ expansion.[10] At intermediate energies, however, one can get a reasonable estimate of such effects from the usual diffractive diagrams of Fig. 10, where $\hat{P}_c$ is in fact the final corrected effective Pomeron for the energy range being considered.

For pp scattering the intermediate vertical lines in Fig. 9 represent nucleons and N^* resonances, as well as background effects. We will use average duality to replace one of these by Regge exchange. In our model this would just be $\hat{P}_c$ exchange so that we finally have the diagram of Fig. 11, which would be the dominant correction at moderate energies and corresponds to single diffractive dissociation (Double diffractive dissociation is not expected to contribute until we reach much higher energies). This diagram is governed by the $\hat{P}_c \hat{P}_c \hat{P}_c$ triple-Regge coupling and gives a contribution to the total cross section of

$$\sigma_D = 2 \int_{\overline{M}_0^2}^{sr} d\overline{M}^2 \int_{-\infty}^{0} dt \, \frac{d\sigma}{dt \, dM^2} \qquad (8.1)$$

where the factor of two arises from the fact that both right- and left-hand

clusters can be replaced by $\hat{P}$ exchange, $sr < \overline{M}^2$ corresponds to the

region of validity of the triple-Regge description (we take $r \simeq 0.2$), and

$$\frac{d\sigma}{dt \, dM^2} = \frac{G(t)}{s^2} \left(\frac{s}{\overline{M}^2}\right)^{2\alpha_{P_c}^{\wedge}(t)} (\overline{M}^2)^{\alpha_{P_c}^{\wedge}(0)} \qquad (8.2)$$

Here $\overline{M}^2 = M^2 - m_p^2 - t$, $\overline{M}_0^2$ is the corresponding threshold value (so

$\overline{M}_0^2 = 0$), and $G(t)$ is proportional to the $\hat{P}_c \hat{P}_c \hat{P}_c$ triple-Pomeron coupling.

We took $G(t)$ from the phenomenological fit made by Dash to the pp $\rightarrow$ pX

data in the triple-Regge region.[14] This gave $G(t) = 2000 \, e^{4t}$.

From Eqs. (8.1) and (8.2) we obtain

$$\sigma_D \simeq L \, s^{\alpha_{P_c}^{\wedge}(0) - 1} \qquad (8.3)$$

where L is an integral over $G(t)$ and has the value $L = 62.9$. We therefore

see that the diffractive contribution cannot change the energy dependence

obtained from the multiperipheral contribution but does increase the overall

magnitude.

In the above calculation we applied local duality down to very low

subenergies when we replaced the N and N[*] with Regge behavior. We

repeated the calculation with Fig. 10(a) evaluated directly and only Fig.

10(b) replaced with Regge behavior. The latter contribution is then given

by Eq. (8.1) but with M_0^2 taken at the πp threshold, which lies roughly halfway between the N and N* (1236) resonance. We found that the results were almost identical with the ones obtained in the previous paragraph.

IX. OVERALL MAGNITUDE OF THE VACUUM-STATE CONTRIBUTION TO THE CROSS SECTION

We will now use our model to calculate the overall magnitude of $\sigma_v = \frac{1}{2}(\sigma_{\bar{p}p} + \sigma_{pp})$, which is essentially the vacuum contribution to the pp cross section. Breaking this up into the multiperipheral and diffractive components we have, from Eq. (8.3),

$$\sigma_v = (\gamma^2_{pp\hat{P}} + L)s^{\alpha_{\hat{P}}(0) - 1} \tag{9.1}$$

for $s < s_R^2 x^2 s_b$. If we compare this with the data at, say, $s = 20$ GeV^2, we have $\gamma^2_{pp\hat{P}} \simeq 110$ (in GeV units) if we take $\alpha_{\hat{P}}(0) = 0.87$. We will now calculate $\gamma^2_{pp\hat{P}}$ from two different starting points.

(1) We will first calculate $\gamma^2_{pp\hat{P}}$ from $\sigma_\omega = \frac{1}{2}(\sigma_{\bar{p}p} - \sigma_{pp})$, which is dominated by ω exchange. Exchange degeneracy then gives

$$\sigma_\omega = \sigma_f = \gamma^2_{ppf}s^{\alpha_f(0) - 1} \tag{9.2}$$

At $s = 20$ GeV^2, for example $\sigma_\omega \simeq 7.5$ mb, which gives $\gamma^2_{ppf} = 84$. From Eqs. (5.7) and (5.9) with $s_R/s_a \simeq m_p^2/m_\rho^2$, we then obtain $\gamma^2_{pp\hat{P}} \simeq 92.4$, which is in fairly good agreement with the empirical value obtained above.

The above calculation assumes that the ω trajectory is unmodified by the inclusion of crossed loops. This is in fact the case in the limit of exact SU(3).[7] If SU(3) is broken, it is no longer exactly true but the modification of the ω still appears to be small compared with that of the f. This is true, for example, in the Chew-Rosenzweig model of ref. 7. Our procedure should therefore continue to be reasonable, at least in some approximate sense.

(2) We will next calculate $\gamma_{\pi\pi\overset{\Lambda}{P}}$ from the ρ resonance with our model

and then use the quark model to relate this to $\gamma_{pp\overset{\Lambda}{P}}$. If we use the finite

energy sum rule (4.5) in the $I_t = 0$ $\pi\pi$ state with $N = 2$ s_a and assume

that $A(t, s)$ is dominated by the ρ resonance with width 0.15 GeV, so that

A is given by Eq. (3.1), we immediately obtain $\gamma_{\pi^+\pi^+f}(0)$. From Eq. (5.7)

we then obtain $\gamma^2_{\pi^+\pi^+\overset{\Lambda}{P}} = 31.2$. If we now use the quark-model result

$\sigma^{pp} = \frac{9}{4}\sigma^{\pi\pi}$, we obtain $\gamma^2_{pp\overset{\Lambda}{P}} = \frac{9}{4}\gamma^2_{\pi^+\pi^+\overset{\Lambda}{P}} = 70.2$, which is somewhat small

compared with the above empirical value.

The most dubious aspect of the above calculation was its assumption

that the ρ resonance dominates in the region $s \lesssim 1$ GeV^2, whereas it is

known that the ϵ peak is also important in this region. One way of

rectifying this situation is to apply our FESR in the s-channel $I_s = 1$

state, where the ϵ is then absent, rather than in the $I_t = 0$ state. The

Regge term on the right side of Eq. (4.5) must now include ρ exchange

as well as f exchange. If we assume that $\gamma_{\pi\pi\rho}$ and $\gamma_{\pi\pi f}$ are related by

exchange degeneracy, however, we again obtain $\gamma_{\pi^+\pi^+f}$, and hence $\gamma_{\pi\pi\overset{\Lambda}{P}}$

from Eq. (5.7). This gives $\gamma^2_{pp\overset{\Lambda}{P}} = \frac{9}{4}\gamma^2_{\pi^+\pi^+\overset{\Lambda}{P}} = 105$, which is in good

agreement with the above empirical value of $\gamma^2_{pp\overset{\Lambda}{P}} = 110$.

X. CONCLUSION

We have used a dual multiperipheral model to calculate a priori the

parameters of the vacuum singularities. We first used a description in

which only a single low-mass cluster with $(\text{mass})^2 \simeq 0.5$ is produced.

This gives a behavior which can be described on the average by a single

effective vacuum singularity at $\alpha_P^\wedge \simeq 0.85$, and is valid below the threshold

for the production of higher clusters. We found that if we included a

second cluster with $(\text{mass})^2 \simeq 1.5$, we obtained a cross section which

flattened out for $s \gtrsim 50 \text{ GeV}^2$. We thus have a parameter-free cross

section which is very similar to the one given by the conventional P + f

description.

The model we have used is, of course, an oversimplification. In

a complete picture we would presumably have more than two clusters

produced, as well as some spread in the mass of each. This would mainly

have the effect of smoothing out the thresholds we obtain but is not expected

to change our main conclusions about the energy dependence of the cross

section. Another simplification was to approximate our Reggeon exchanges

with a single effective trajectory $\alpha_e = 0.25 + t$. In a more correct treatment

we should have a Reggeon with $\alpha = 0.5 + t$ and a pion with $\alpha = t$ coming

in explicitly.

We have used a rather simple-minded multiperipheral model in which

threshold effects had to be put in by hand through a factor x^{-j}. In a more

complete treatment they would arise naturally. This happens, for example, in the pion-exchange model (see Appendix A), and would also occur in any other model in which the momentum transfers are limited.

We have neglected anti-baryon production in our model, which may play an important role for $s \gtrsim 200 \text{ GeV}^2$. Duality schemes generally have problems when they are applied to baryons, however, and so our framework may have to be modified in this energy region.

ACKNOWLEDGMENTS

APPENDIX A.   THRESHOLD FACTORS IN AN EXPLICIT PION-EXCHANGE MODEL

We will now see explicitly how threshold factors, such as the one

in Eq. (3.8), arise in the case of the Amati-Bertocchi-Fubini-Stanghellini-

Tonin (ABFST) pion-exchange model.[1, 18] Similar factors are expected

to arise in a Reggeon-exchange model.

It is possible to partially diagonalize the ABFST equation by using

the transform

$$A_\lambda(\tau_1, \tau_2) = \int_{4m_\pi^2}^{\infty} ds\, e^{-(\lambda+1)\theta(s, \tau_1, \tau_2)} A(s, \tau_1 \tau_2) \quad (A.1)$$

of the forward off-shell $\pi\pi$ scattering amplitude $A(s, \tau_1, \tau_2)$, where

$\sqrt{\tau_1}$ and $\sqrt{\tau_2}$ are the off-shell pion masses and

$$e^{-\theta(s, \tau_1, \tau_2)} = \frac{2\sqrt{-\tau_1}\sqrt{-\tau_2}}{(s - \tau_1 - \tau_2) + \left[(s - \tau_1 - \tau_2)^2 - 4\tau_1\tau_2\right]^{1/2}} \cdot \quad (A.2)$$

The forward ABFST equation then takes on the form[18]

$$A_\lambda(\tau_1, \tau_2) = V_\lambda(\tau_1 \tau_2) + \frac{1}{16\pi^3(\lambda+1)} \int_{-\infty}^{0} \frac{d\tau'}{(m_\pi^2 - \tau')^2} V_\lambda(\tau_1, \tau') A_\lambda(\tau', \tau_2) \cdot \quad (A.3)$$

If we assume the production of a single cluster, Eq. (3.1) gives

$$V(s, \tau_1, \tau_2) = v(\tau_1) v(\tau_2) \delta(s - s_a). \quad (A.4)$$

assuming factorization, which, as we saw from Eq. (2.3), is demanded
by duality.

Suppose we assume that the off-shell behavior is such that the
τ_1, τ_2 are limited. This would be true, for example, with a Benecke-Dürr
off-shell factor, which works so well in accounting for pion production
in the single pion-exchange model. Then, if $s_a \gg \tau_1$, τ_2, we can make
the approximation

$$e^{-\theta(s, \ \tau_1, \ \tau_2)} \simeq \sqrt{-\tau_1} \ \sqrt{-\tau_2}/s_a \qquad (A.5)$$

Eq. (A.3) can now be solved exactly and gives

$$A_\lambda(\tau_1, \ \tau_2) = V_\lambda(\tau_1, \ \tau_2)/D_\lambda \qquad (A.6)$$

where

$$D_\lambda = 1 - \frac{1}{16\pi^3(\lambda+1)} \int_{-\infty}^{0} \frac{d\tau'}{(m_\pi^2 - \tau')^2} \ V_\lambda(\tau', \ \tau') \qquad (A.7)$$

and

$$V_\lambda(\tau_1, \ \tau_2) = \nu(\tau_1) \nu(\tau_2) s_a^{-\lambda-1} (\sqrt{-\tau_1} \ \sqrt{-\tau_2})^{\lambda+1} \qquad (A.8)$$

The simplest kind of off-shell behavior we can have which at the
same time limits τ_1 and τ_2 corresponds to taking

$$\nu(\tau) = \nu_0 \, \theta(\tau + T) \tag{A.9}$$

where θ is the usual step function. If we neglect m_π^2, Eq. (A.7) then reduces to

$$D_\lambda = 1 - \frac{\nu_0^2 s_a^{-1}}{16\pi^3(\lambda + 1)\lambda} \left(\frac{s_a}{T}\right)^{-\lambda} . \tag{A.10}$$

This basically has the structure of Eqs. (3.12) and (3.8) if we identify λ with j, except for the extra factor of λ in the denominator, which arises only because we set $m_\pi^2 \simeq 0$. Another possible form is

$$\nu(\tau) = \nu_0 e^{\tau/2T} . \tag{A.11}$$

If we again neglect m_π^2 we obtain

$$D_\lambda = 1 - \frac{\nu_0^2 s_a^{-1} \Gamma(\lambda)}{16\pi^3(\lambda + 1)} \left(\frac{s_a}{T}\right)^{-\lambda} \tag{A.12}$$

which also has the same kind of structure as Eqs. (3.12) and (3.8).

APPENDIX B.   ALTERNATIVE CALCULATION OF $\hat{P}$

We will now present an alternative calculation in which we first

sum over the uncrossed loops to obtain the amplitude A_f of Sec. IV, which

is dominated by f exchange at high energies.   We then treat A_f itself as

a cluster linked by the crossed propagators of Eq. (2.1).   This is similar

in spirit to the treatment of Chan et al.[6]   We do not, however, go to the

ultimate duality limit of actually replacing A_f by a Reggeon.   We have already

seen that the resonance nature of the clusters plays an important role in

determining the nature of the behavior of the cross section.

If we apply Eqs. (3.5), (3.8), (3.10), (3.11), (3.12) and (5.1) to

$\pi\pi$ scattering, we can write

$$A_{\hat{P}}(t, j) = \frac{A_f(t, j)}{1 - [K_{\hat{P}} - K_f(t, j)]A_f(t, j)} \qquad (B.1)$$

where $K_{\hat{P}}$ and K_f are given by Eq. (3.8) with $k = k_{\hat{P}}$ and k_f corresponding

to Eqs. (4.3) and (5.2), and A_f is given by Eqs. (3.8), (3.10), (3.11),

(3.12) and (4.1).   If we expand the denominator of Eq. (B.1) we obtain

the diagrams of Fig. 12.   The A_f now play the role of generalized clusters

which are linked by crossed Reggeon lines giving the $(K_{\hat{P}} - K_f)$ factors.

Chan et al   essentially replaced A_f by a simple Regge pole.   This

approximation is rather crude.   To take better account of the structure of

A_f we assumed instead that it is dominated by an a-cluster for $s \lesssim 1$ GeV^2

and by f-exchange for $s \gtrsim 1$ GeV^2.   Using Eq. (2.3), we then have

$$A_f(t, j) = \gamma^2_{\pi\pi f}(t) \left\{ F_a(t)s_a^{-j-1} + \frac{1}{j - \alpha_f} N^{\alpha_f - j} \right\} \quad (B.2)$$

and $N \simeq 1 \text{ GeV}^2$. Eq. (B.1) now gives rise to an output pole at the point

$j = \alpha_P^\Lambda$ where the denominator vanishes. If we calculate the corresponding

residue $\gamma^2_{\pi\pi P}$ we obtain $\alpha_P^\Lambda(0) = 0.88$ and $\gamma^2_{\pi\pi P}/\gamma^2_{\pi\pi f}(0) = 1.54$ with

Eq. (4.7) for F_a (Prescription B). These results are almost identical

with Eqs. (5.6) and (5.7).

REFERENCES

[1] D. Amati, A. Stanghellini and S. Fubini, Nuovo Cimento 26, 896 (1962); L. Bertocchi, S. Fubini, and M. Tonin, ibid. 25, 626 (1962).

[2] D. R. Avalos and B. R. Webber, Phys. Rev. D4, 3313 (1971); D. Tow, Phys. Rev. D2, 154 (1970); G. F. Chew, T. Rogers and D. Snider, Phys. Rev. D2, 765 (1970).

[3] Huan Lee, Phys. Rev. Lett. 30, 719 (1973).

[4] G. Veneziano, Phys. Lett. 43B, 413 (1973).

[5] Chan Hong-Mo and J. E. Paton, Phys. Lett. 46B, 228 (1973).

[6] Chan Hong-Mo, J. E. Paton and Tsou Sheung Tsun, Nucl. Phys. B86, 479 (1975); Chan Hong-Mo, J. E. Paton, Tsou Sheung Tsun and Ng Sing Wai, Nucl. Phys. B92, 13 (1975); N. A. Sakai, Nucl. Phys. B99, 167 (1975).

[7] C. Rosenzweig and G. F. Chew, Phys. Lett. 58B, 93 (1975); Nucl. Phys. B104, 290 (1976); C. Schmid and C. Sorensen, Nucl. Phys. B96, 209 (1975).

[8] L. A. P. Balázs, Phys. Lett. 61B, 187 (1976).

[9] J. E. Paton and Chan Hong-Mo, Nucl. Phys. B10, 516 (1969).

[10] G. Veneziano, Nucl. Phys. B74, 365 (1974); Phys. Lett. 52B, 220 (1974).

[11] L. A. P. Balázs, Phys. Lett. 29B, 228 (1969); Phys. Rev. D2, 999 (1970).

[12] G. F. Chew, M. L. Goldberger and F. E. Low, Phys. Rev. Lett. $\underline{22}$, 208 (1969).

[13] R. D. Field and G. C. Fox, Nucl. Phys. $\underline{B80}$, 367 (1974); D. P. Roy and R. G. Roberts, Nucl. Phys. $\underline{B77}$, 240 (1974); L. A. P. Balázs, Phys. Rev. $\underline{D11}$, 1071 (1975); T. Inami and R. G. Roberts, Nucl. Phys. $\underline{B93}$, 497 (1975).

[14] J. Dash, Phys. Rev. $\underline{D9}$, 200 (1974); N. Bali and J. Dash, Phys. Rev. $\underline{D10}$, 2102 (1974).

[15] R. Carlitz, M. B. Green and A. Zee, Phys. Rev. $\underline{D4}$, 3439 (1971).

[16] G. F. Chew and D. Snider, Phys. Lett. $\underline{31B}$, 75 (1970); G. F. Chew and J. Koplik, Phys. Lett. $\underline{48B}$, 221 (1974); J. Dash, Phys. Lett. $\underline{61B}$, 199 (1976).

[17] L. A. P. Balázs, Phys. Lett. $\underline{35B}$, 519 (1971); Phys. Rev. $\underline{D4}$, 2364 (1971).

[18] S. Nussinov and J. Rosner, J. Math Phys. $\underline{7}$, 1670 (1966).

FIGURE CAPTIONS

Fig. 1:   Multiperipheral model for the production of clusters.

Fig. 2:   Two-body absorptive part given by Fig. 1.

Fig. 3:   Uncrossed (planar) quark-duality diagram.

Fig. 4:   Nonplanar quark-duality diagram with crossed and uncrossed

           loops.

Fig. 5:   Average duality relation between cluster (a) and Reggeon (b).

Fig. 6:   Absorptive part A arising from the production of a-clusters.

Fig. 7:   Function B obtained after factoring out end-clusters as in

           Eq. (3.5).

Fig. 8:   Function $B = B_P$ for a- and b-cluster production in terms

           of the function $B = B_P^\Lambda$ for a-cluster production.

Fig. 9:   The vacuum-state contribution to the pp total cross section.

Fig. 10:   Diffractive contributions to the absorptive part.

Fig. 11:   Triple-Pomeron contribution to the absorptive part.

Fig. 12:   Absorptive part with crossed loops linking the functions

           A_f generated by summing all uncrossed diagrams.

Fig. 1

Fig. 2

Fig. 3

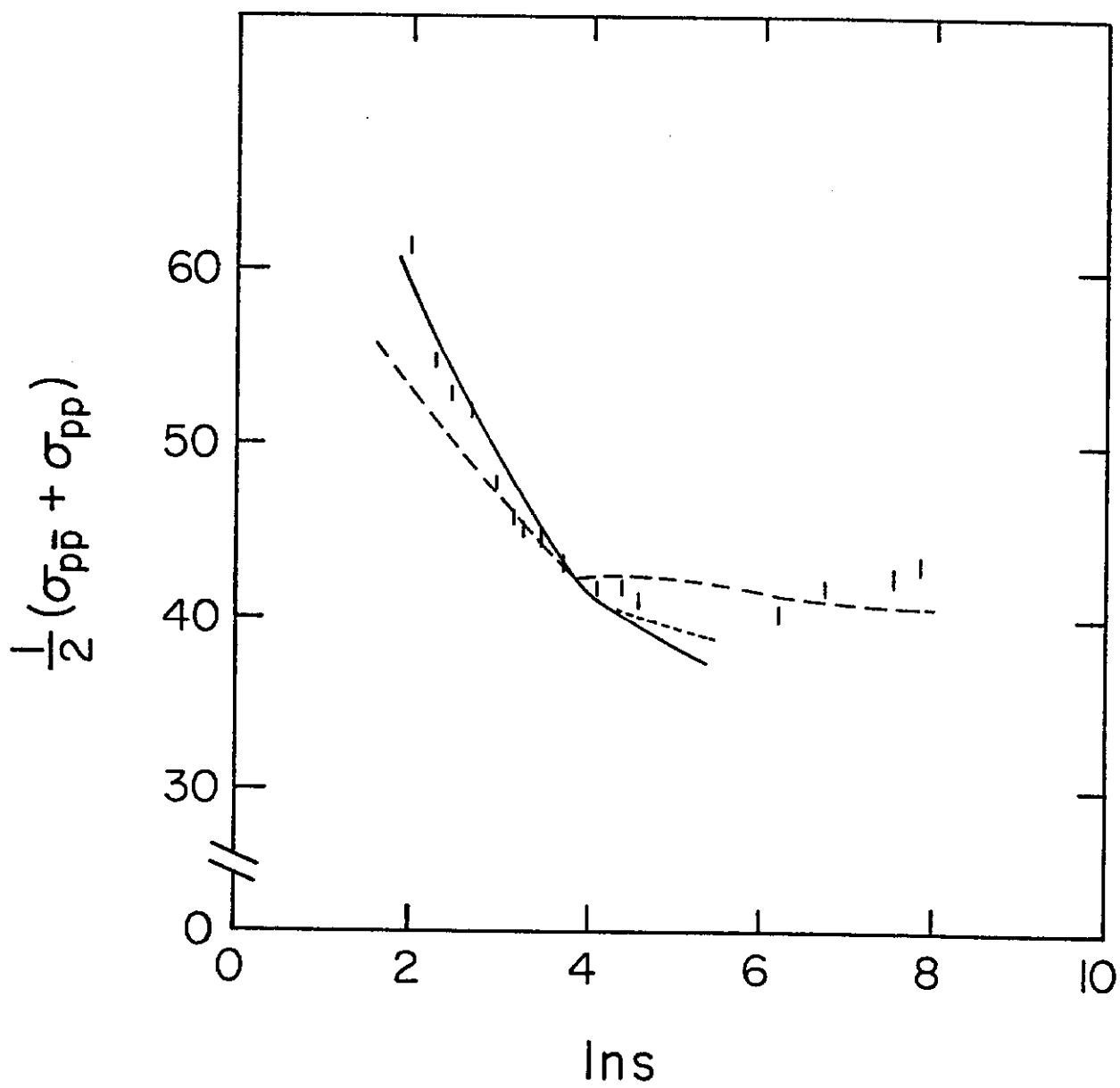
Fig. 4

Fig. 5

(a)   (b)

Fig. 6

Fig. 7

Fig. 8

Fig. 9

Fig. 10

Fig. 11

Fig. 12